Journal of Physics: Conference Series

OPEN ACCESS

Quantum Monte Carlo with non-local chiral interactions

To cite this article: A Roggero *et al* 2014 *J. Phys.: Conf. Ser.* **527** 012003

View the article online for updates and enhancements.

You may also like

- Spin-orbit excitations of quantum wells
A. Ambrosetti, J. M. Escartín, E. Lipparini et al.
- Applications of quantum Monte Carlo methods in condensed systems
Jindich Koloren and Lubos Mitas
- Compact gamma detectors based on FBK SiPMs for a Ps Time Of Flight apparatus
E Mazzuca, M Benetti, S Mariazzi et al.

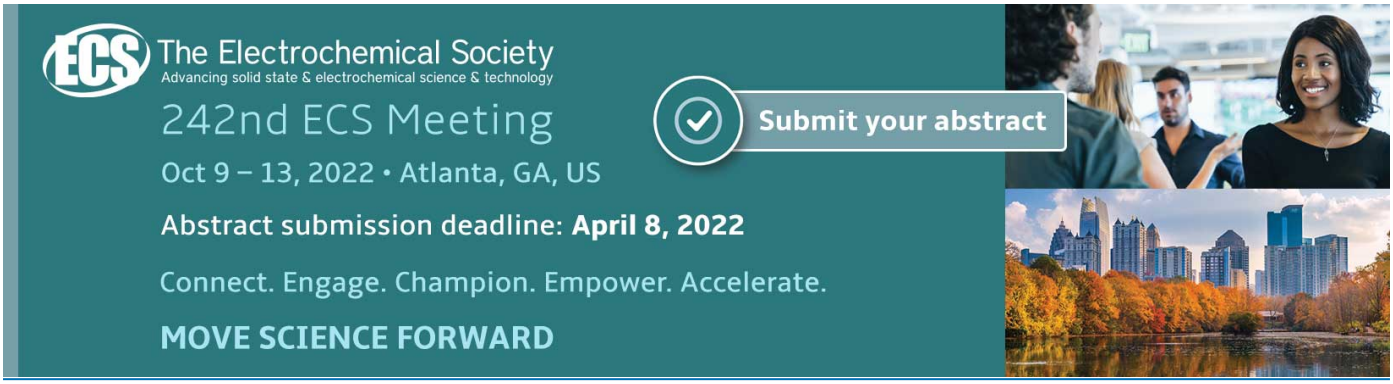

This content was downloaded from IP address 93.40.240.224 on 14/03/2022 at 17:58

Journal of Physics: Conference Series **527** (2014) 012003 doi:10.1088/1742-6596/527/1/012003

Quantum Monte Carlo with non–local chiral interactions

A Roggero[1,2], A Mukherjee [3], F Pederiva[1,2]

[1] Physics Department, University of Trento, via Sommarive 14, I-38123 Trento, Italy
[2] INFN-TIFPA, Trento Institute for Fundamental Physics and Applications
[3] ECT*, Villa Tambosi, I-38123 Villazzano (Trento), Italy

E-mail: roggero@science.unitn.it,mukherjee@ectstar.eu,pederiva@science.unitn.it

Abstract. Quantum Monte Carlo methods have been used very successfully to calculate the ground state properties of a variety of nuclear and other strongly interacting many body systems. An exciting recent development in low energy nuclear physics is the formulation of nuclear Hamiltonians based on the symmetries of quantum chromodynamics via chiral effective field theory. However, the usual coordinate space based quantum Monte Carlo implementation is unsuitable for these Hamiltonians due to the presence of non-localites. Here we report on our recent work in developing a new quantum Monte Carlo algorithm suitable for these non-local Hamiltonians, and present some results for pure neutron matter.

1. Introduction

Predicting the properties of nuclei from the underlying theory of strong interactions viz. quantum chromodynamics (QCD) is one of the long standing goals of nuclear physics. Chiral effective field theory (χ-EFT) serves as a bridge between QCD and low energy nuclear physics by providing a systematic expansion for the nuclear forces based on the symmetries and on the symmetry breakings of QCD [1, 2, 3]. Chiral interactions have already been employed in calculations of nuclear structure and reactions of light and medium-mass nuclei [4, 5, 6, 7, 8, 9, 10, 11, 12, 13, 14, 15, 17, 16, 18, 19], and infinite matter [20, 21, 22, 23, 24, 25, 26].

Amongst the available non-perturbative methods for strongly interacting systems, quantum Monte Carlo (QMC) methods have proven to be extremely accurate for a variety of systems [27, 28]. In fact, some of the most accurate calculations for light nuclei and neutron matter were performed using continuum diffusion based QMC methods, i.e., nuclear Green's function Monte Carlo (GFMC) and auxiliary field diffusion Monte Carlo (AFDMC) [29, 30, 31, 32], in conjunction with the semi phenomenological *local* Argonne-Urbana family of nuclear forces [33, 34]. On the other hand, the interactions obtained from chiral EFT are, in general, *non-local*, and hence are difficult to incorporate in standard continuum QMC methods [1].

In this work, we report our calculations with a non–local chiral interaction in which a proper QMC algorithm is used. The interaction we use is the recently developed chiral $\mathrm{NNLO_{opt}}$ interaction [35], which fits the experimantal phase–shifts at $\chi^2 \sim 1$ for laboratory energies less

[1] See however [25] for a recent attempt to incorporate chiral interactions in continuum QMC by removing non-localities up to next-to-next-to-leading order (NNLO).

Content from this work may be used under the terms of the Creative Commons Attribution 3.0 licence. Any further distribution of this work must maintain attribution to the author(s) and the title of the work, journal citation and DOI.
Published under licence by IOP Publishing Ltd

than 125 MeV. However, the contribution from the three nucleon forces is smaller with this parametrization than with the previous ones.

In the next section we present the QMC method and then we will present an application to neutron matter.

2. Method

Quantum Monte Carlo methods solve the Schroedinger equation for the ground state by looking at the long τ solution of the imaginary–time equation:

$$-\frac{\partial}{\partial\tau}|\Psi(\tau)\rangle = H|\Psi(\tau)\rangle = (K+V)|\Psi(\tau)\rangle \tag{1}$$

where K and V are respectively kinetic and potential parts of the total Hamiltonian H. equation (1) can be recast into the integral equation:

$$\langle\mu|\Psi(\tau+\Delta\tau)\rangle = \int d\nu\langle\mu|G_{\Delta\tau}|\nu\rangle\langle\nu|\Psi(\tau)\rangle \tag{2}$$

where we employed a (continuous) complete sets of states $|\nu\rangle$ and $|\mu\rangle$ for convenience and G is the Green's function of equation (1), the so–called imaginary-time propagator. By repeatedly integrating (2), starting from some initial ansatz for the wave-function, we will project to the eigenstate of H with the lowest eigenvalue.

Conventional QMC methods formulated in coordinate space ($\nu,\mu \equiv \mathbf{R}$) rely on the fact that for small imaginary–time step $\Delta\tau$ we have the factorization

$$\langle\mathbf{R}'|G_{\Delta\tau}|\mathbf{R}\rangle = G_{\Delta\tau}(\mathbf{R}',\mathbf{R}) \approx G^d_{\Delta\tau}(\mathbf{R}',\mathbf{R})G^b_{\Delta\tau}(\mathbf{R}') + O(\Delta\tau^2) \tag{3}$$

where $G^d_{\Delta\tau}(\mathbf{R}',\mathbf{R})$ is the free-particle Green's function coming from the kinetic energy term K and $G^b_{\Delta\tau}(\mathbf{R}')$ takes into account the effect of interactions V . Now if $G^d_{\Delta\tau}(\mathbf{R}',\mathbf{R})$ is positive–definite we can interpret it as a probability and use stochastic methods to integrate (2). This scheme however cannot be followed in the general case where the interaction is non–local in coordinate space: $\langle\mathbf{R}'|V|\mathbf{R}\rangle \neq V(\mathbf{R}')\delta(\mathbf{R}'-\mathbf{R})$. In this case in fact transitions to new states is controlled also by the potential and finding efficient ways to perform the sampling becomes a challenging task (cf. [52]). Unfortunately in general interactions coming from χ–EFT belong to this class [1, 2, 3].

These problems associated with non–local potentials are however essentially connected to fact that we are working in a continuous single–particle basis. Let us then take a finite set $\mathcal{S}$ of sp states of size $\mathcal{N}_s$ and consider a general second–quantized fermionic Hamiltonian which includes only two–body interactions

$$H = \sum_{i\in\mathcal{S}} \epsilon_i a_i^\dagger a_i + \sum_{abij\in\mathcal{S}} V_{ij}^{ab} a_a^\dagger a_b^\dagger a_i a_j \ , \tag{4}$$

where $a_i^\dagger$ creates a particle in the single-particle (sp) state labeled by i (i is a collective label for all sp quantum numbers) and the V_{ij}^{ab} are general two-body interaction matrix elements.

The resulting many–body Hilbert space would be spanned by the full set of N–particle Slater determinants that can be generated using the sp orbitals $i \in \mathcal{S}$. At this point we want to solve for the ground–state of the system by repeatedly applying a projection operator like

$$\begin{aligned}\langle\mathbf{m}|P|\mathbf{n}\rangle \equiv \langle\mathbf{m}|G_{\Delta\tau}|\mathbf{n}\rangle &= 1-\Delta\tau\,(H-E_T)|\mathbf{n}\rangle \\ &= \delta_{\mathbf{m},\mathbf{n}} - \Delta\tau\langle\mathbf{m}|H-E_T|\mathbf{n}\rangle\end{aligned} \tag{5}$$

where E_T is just an energy shift used to preserve the norm of the solution.

Since our final purpose is to interpret the off–diagonal terms in (5) as probabilities, we need the matrix elements $\langle \mathbf{m}|P|\mathbf{n}\rangle \geq 0$ (or equivalently $\langle \mathbf{m}|H|\mathbf{n}\rangle \leq 0$). In general however P will have negative–matrix elements which will cause problems, this is once again a manifestation of the sign–problem.

In principle, one can still produce a stochastic evolution absorbing the signs into the renormalization factor and sampling off-diagonal moves using $|\langle \mathbf{m}|P|\mathbf{n}\rangle|$, but this is accompanied by an exponential decay of the signal to noise ratio as a function of the projection time $\tau = M\Delta\tau$. Recently it was shown that by employing an annihilation step in the evolution this problem can be substantially alleviated [36, 37, 38]. At the end however these algorithms have still an exponential scaling with system–size, though with a reduced exponent.

In CIMC we instead deal with the sign–problem in a way which is somewhat similar to standard coordinate–space QMC: we will use an initial ansatz Φ_T for the ground–state wave–function and use that to constrain the random walk in a region of the many–body Hilbert space where $\langle \mathbf{m}|P|\mathbf{n}\rangle \geq 0$ is satisfied. In order to this scheme to be practical one needs a systematic way for reducing the bias coming from this approximation, e.g. we want the bias to go to zero as the ansatz Φ_T goes towards the ground–state Ψ_0. That's exactly what is done in coordinte-space fixed–node QMC simulations.

Following the work in [39, 40] we define a new Hamiltonian $\mathcal{H}$, whose off–diagonal matrix elements are given by

$$\langle \mathbf{m}|\mathcal{H}|\mathbf{n}\rangle = \begin{cases} 0 & \mathfrak{s}(\mathbf{m},\mathbf{n}) > 0 \\ \langle \mathbf{m}|H|\mathbf{n}\rangle & \text{otherwise} \end{cases} , \tag{6}$$

while the diagonal terms are

$$\langle \mathbf{n}|\mathcal{H}|\mathbf{n}\rangle = \langle \mathbf{n}|H|\mathbf{n}\rangle + \sum_{\substack{\mathbf{m}\neq\mathbf{n} \\ \mathfrak{s}(\mathbf{m},\mathbf{n})>0}} \mathfrak{s}(\mathbf{m},\mathbf{n}) . \tag{7}$$

where $\mathfrak{s}(\mathbf{m},\mathbf{n}) = \Phi_T(\mathbf{m})\langle \mathbf{m}|H|\mathbf{n}\rangle/\Phi_T(\mathbf{n})$, and a new propagator

$$\langle \mathbf{m}|\mathcal{P}|\mathbf{n}\rangle = \delta_{\mathbf{m},\mathbf{n}} - \Delta\tau\Phi_T(\mathbf{m})\langle \mathbf{m}|\mathcal{H} - E_T|\mathbf{n}\rangle/\Phi_T(\mathbf{n}) . \tag{8}$$

Now the propagator $\mathcal{P}$ is, by construction, free from the sign–problem and performing the corresponding random–walk allows us to filter the state $\Phi_T(\mathbf{n})\phi_0(\mathbf{n})$, where now $\phi_0(\mathbf{n})$ is the ground–state of the hamiltonian $\mathcal{H}$. The ground–state energy ϵ obtained following this procedure is a strict upper bound for the true ground–state energy E_{gs} of the true hamiltonian H and, moreover, this upper bound is tighter than the variational upper–bound provided by $\langle \Phi_T|H|\Phi_T\rangle$ [39, 40, 41].

Up to now we have just discussed real–symmetric hamiltonian matrices but in the case of χ-EFT interactions in momentum–space we have to deal with a complex–hermitian matrix. The extension to this more general case of equations (6)-(8) can be actually performed while preserving all the favorable properties of the method discussed so far: we replace $\mathfrak{s}(\mathbf{m},\mathbf{n})$ in equation (6) and equation (7) with

$$\mathfrak{s}'(\mathbf{m},\mathbf{n}) = \frac{\mathcal{R}e\left[\Phi_T^*(\mathbf{m})\langle \mathbf{m}|H|\mathbf{n}\rangle\Phi_T(\mathbf{n})\right]}{|\Phi_T(\mathbf{n})|^2} , \tag{9}$$

where $\mathcal{R}e$ selects the real part, and define the propagator

$$\langle \mathbf{m}|\mathcal{P}'|\mathbf{n}\rangle = \delta_{\mathbf{m},\mathbf{n}} - \Delta\tau\frac{\mathcal{R}e\left[\Phi_T^*(\mathbf{m})\langle \mathbf{m}|\mathcal{H} - E_T|\mathbf{n}\rangle\Phi_T(\mathbf{n})\right]}{|\Phi_T(\mathbf{n})|^2} . \tag{10}$$

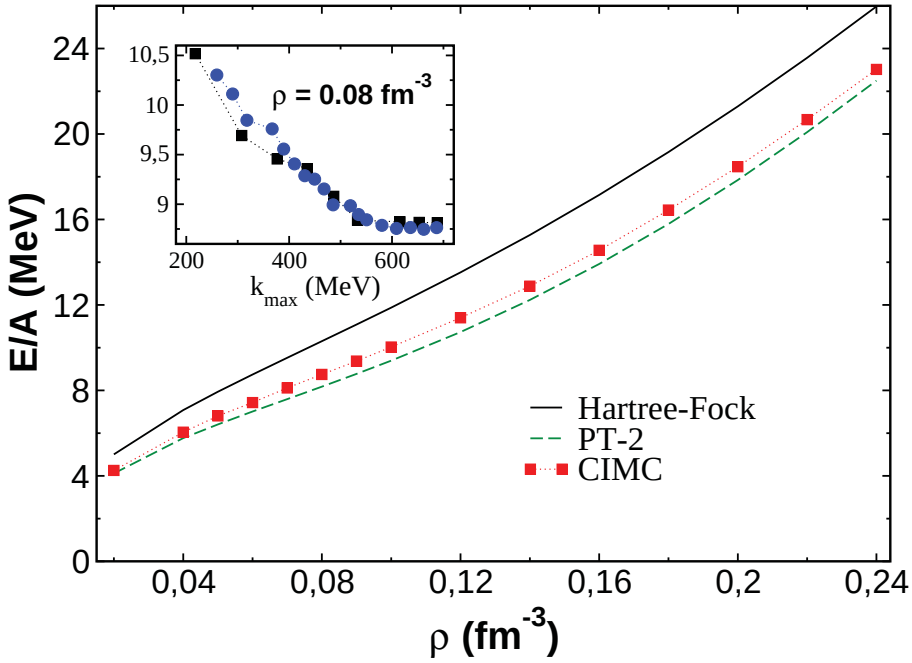

Figure 1. (Color online) The EoS of pure neutron matter (66 neutrons) using the same χ-EFT interaction with different methods: red squares - our Monte Carlo results, black solid line Hartree-Fock, green dashed lines PT-2. The inset shows the convergence of our energies as a function of $k_{\max}$ at $\rho = 0.08$ fm^{-3} for 14 (black squares) and 66 (blue circles) particles. The dotted lines are a guide to the eye.

The proofs of upper bound properties is analogus to the one in the real case and will be reported elsewhere [42].

Finally, to assure the success of the proposed method a good choice for the importance function $|\Phi_T\rangle$ is crucial, we need a wave–function flexible enough to account for the relevant correlations in the system and that at the same time can be evaluated sufficiently quickly on a computer. In many strongly–interacting systems coupled–cluster theory provide an ansatz that fulfills the first criterion. In [51] we showed how to evaluate the overlaps $\langle \mathbf{n}|\Phi_T\rangle$ in a computationally efficient way in the so–called coupled cluster doubles (CCD) approximation. Extensions to include singles (CCSD) and triples (CCSDT) corrections, useful for treating inhomogeneous systems or many–body interactions, are straightforward.

3. Neutron matter in momentum–space

In this work we choose for the sp basis states the eigen–states of momentum and the z components of spin and iso–spin. Calculations are performed at fixed density ρ by putting A nucleons in a cubic box of size $L^3 = A/\rho$ with periodic boundary conditions. The finiteness of the box requires the sp states to lie on a cubic lattice in momentum space with lattice constant $l = 2\pi/L$. This scale imposes thus an infra–red (IR) cut off in our scheme, and in order to obtain a finite basis we impose an additional ultra–violet (UV) cut off $k_{\max}$ so that only sp states with $k_i^2 \leq k_{\max}^2$ are included. A sequence of calculations with increasing $k_{\max}$ and decreasing l need to be performed till convergence is reached.

In the inset of figure 1 we plot the energy per particle as a function of the UV cut off $k_{\max}$ at $\rho = 0.08$ fm^{-3} for for both 14 and 66 neutrons, at all densities considered in this work we found the same smooth behaviour. The CIMC calculations are considered to have converged

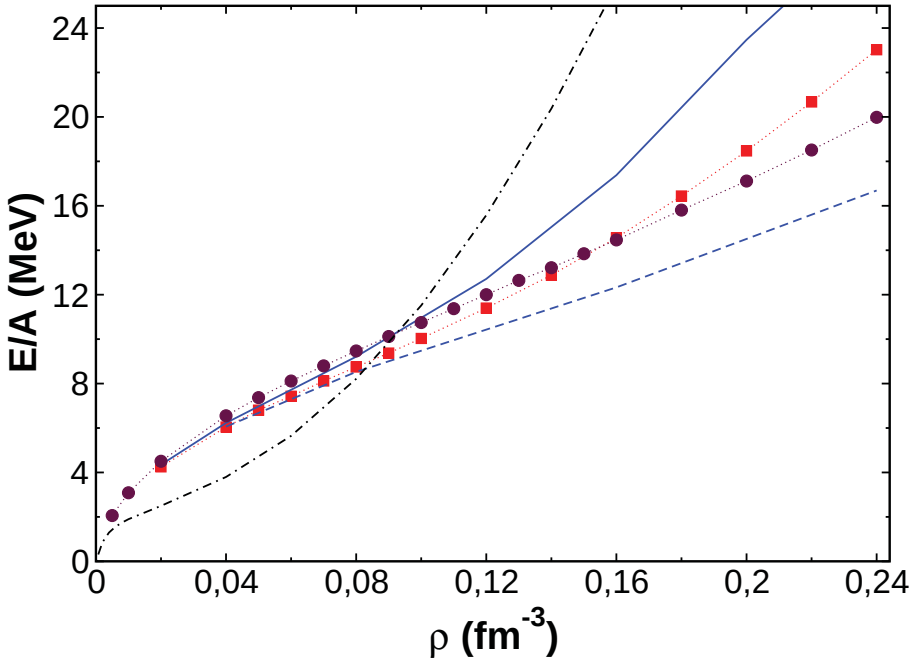

Figure 2. (Color online) The EoS of pure neutron matter: red squares - our results (66 neutrons), brown circles - AFDMC EoS with the 2b AV8' [44], blue dashed line - APR EoS with the 2b AV18 [43], blue solid line - APR EoS with the 2b AV18 + 3b UIX [43], black dashed dotted line - NL3 EoS [46].

when the difference in energy between two successive values of $k_{\max}$ is less than the statistical error ($\approx 10-25$ KeV at convergence).

Interestingly UV convergence is obtained for values $k_{\max}-k_f$ 450 MeV (where k_f is the Fermi momentum) which is comparable to the momentum–cutoff at 500 MeV in the N2LO interaction. We find this to be the case for all densities considered.

In figures 1 and 2 we show our results for pure neutron matter. In figure 1 we compare them with Hartree-Fock (HF) and 2nd order perturbation theory (PT-2) calculations employing the same interaction. As is apparent neutron matter with this chiral interaction is pretty much perturbative, with PT-2 numbers consistently overestimating the binding energy but still quite close to the non–perturbative answer given by CIMC .

In figure 2 we include the variational APR EoSs (two body - AV18 and two plus three body - AV18+UIX interactions) [43] and the AFDMC EoS (two body - AV8′ interaction) [44] obtained with realistic interactions fitting the NN phase–shifts data. Most computer simulations of supernovae use phenomenological EoSs based typically on the liquid drop model, the most popular being the Lattimer-Swesty EoS [45], or on relativistic mean field theory [46, 47, 48, 49, 50]. As a prototype of such an EoS we have included the results from the NL3 EoS [46].

As can be seen the calculations based on microscopic Hamiltonians are consistent (within about 10%) at low densities ($\lesssim 0.1$ fm^{-3}) and other many–body calculations with realistic interactions [24, 25, 22, 26, 21, 20] are also consistent with the ones shown in the figure in this density range.

Phenomenological approaches as the NL3 model on the other hand show a completely different behaviour even at very low densities. This strong deviation of predictions obtained from these popular phenomenological models from the results obtained from microscopic calculations was

also pointed out recently in [26] in the context of χ-EFT interactions.

4. Conclusion

In conclusion, we reported the first quantum Monte Carlo calculations with non-local chiral interactions. In this preliminary applications we find, unsurprisingly, that the equation of state of neutron matter at low densities is reasonably model independent as long as the interaction used is fit to the low energy scattering phase shifts.

The QMC method described in this paper is quite general and can be used for nuclear matter and finite nuclei, and with three body forces. This work paves the way to a systematic non–perturbative study of chiral–forces in all this regimes. Work in these directions is in progress.

Acknowledgments

We are grateful to G Hagen and T Papenbrock for sharing their CCD code and benckmarks with us, and to A Ekström, G Hagen and T Papenbrock for sharing the numerical program for the chiral interaction. A Mukherjee would like to thank W Weise for numerous fruitful discussions. Computations were performed at the Open Facilities at the Lawrence Livermore National Laboratory.

References

[1] Epelbaum E, Hammer H W, and Meißner U G 2009 *Rev. Mod. Phys.* **81** 1773
[2] Machleidt R and Entem D R 2011 *Phys. Rep.* **503** 1
[3] Hammer H W, Nogga A, and Schwenk 2013 *Rev. Mod. Phys.* **85** 197
[4] Kalantar-Nayestanaki N, Epelbaum E, Messchendorp J G, and Nogga A 2012 *Rep. Prog. Phys.* **75** 016301
[5] Barrett B R, Navrátil P, and Vary J P 2013 *Prog. Part. Nucl. Phys.* **69** 131
[6] Roth R, Langhammer J, Calci A, Binder S, and Navrátil P 2011 *Phys. Rev. Lett.* **107** 072501
[7] Roth R, Binder S, Vobig K, Calci A, Langhammer J, and Navrátil P 2012 *Phys. Rev. Lett.* **109** 052501
[8] Hergert H, Bogner S K, Binder S, Calci A, Langhammer J, Roth R, and Schwenk A 2013 *Phys. Rev. C* **87** 034307
[9] Epelbaum E, Krebs H, Lee D, and Meißner U G 2009 *Eur. Phys. J. A* **40** 199
[10] Epelbaum E, Krebs H, Lee D, and Meißner U G 2010 *Phys. Rev. Lett.* **104** 142501
[11] Epelbaum E, Krebs H, Lee D, and Meißner U G 2011 *Phys. Rev. Lett.* **106** 192501
[12] Epelbaum E, Krebs H, Lähde T A, Lee D, and Meißner U G 2013 *Phys. Rev. Lett.* **110** 112502
[13] Hagen G, Hjorth-Jensen M, Jansen G R, Machleidt R, and Papenbrock T 2012 *Phys. Rev. Lett.* **109** 032502
[14] Hagen G, Hjorth-Jensen M, Jansen G R, Machleidt R, and Papenbrock T 2012 *Phys. Rev. Lett.* **108** 242501
[15] Otsuka T, Suzuki T, Holt J D, Schwenk A, and Akaishi Y 2010 *Phys. Rev. Lett.* **105** 032501
[16] Holt J D, Menéndez J, and Schwenk A 2013 *J. Phys. G* **40** 075105
[17] Holt J D, Otsuka T, Schwenk A, and Suzuki T 2012 *J. Phys. G* **39** 085111
[18] Somà V, Barbieri C, and Duguet T 2013 *Phys. Rev. C* **87** 011303
[19] Wienholtz F *et al.* 2013 *Nature* **498** 7454
[20] Kaiser N, Fritsch S, and Weise W 2002 *Nucl. Phys. A* **697** 255
[21] Holt J W, Kaiser N, and Weise W 2013 *Phys. Rev. C* **87** 014338
[22] Tews I, Krüger T, Hebeler K, and Schwenk A 2013 *Phys. Rev. Lett.* **110** 032504
[23] Baardsen G, Ekström A, Hagen G, and Hjorth-Jensen M 2013 *Phys. Rev. C* **88** 054312
[24] Hagen G, Papenbrock T, Ekström A, Wendt K A, Baardsen G, Gandolfi S, Hjorth-Jensen M, and Horowitz C J 2014 *Phys. Rev. C* **89** 014319
[25] Gezerlis A, Tews I, Epelbaum E, Gandolfi S, Hebeler K, Nogga A, and Schwenk A 2013 *Phys. Rev. Lett.* **111** 032501
[26] Krüger T, Tews I, Hebeler K, and Schwenk A 2013 *Phys. Rev. C* **88** 025802
[27] Kalos M H and Whitlock P A 2009 *Monte Carlo methods* (Wiley-VCH)
[28] Foulkes W M C, Mitas L, Needs R J, and Rajagopal G 2001 *Rev. Mod. Phys.* **73** 33
[29] Pudliner B S, Pandharipande V R, Carlson J, Pieper S C, and Wiringa R B 1997 *Phys. Rev. C* **56** 1720
[30] Pieper S C 2008 *Riv. Nuovo Cimento* **31** 2008
[31] Gandolfi S, Illarionov A Y, Schmidt K E, Pederiva F, and Fantoni S 2009 *Phys. Rev. C* **79** 054005
[32] Gezerlis A and Carlson J 2010 *Phys. Rev. C* **81** 025803
[33] Wiringa R B, Stoks V G J, and Schiavilla R 1995 *Phys. Rev. C* **51** 38

[34] Pieper S C, Pandharipande V R, Wiringa R B, and Carlson J 2001 *Phys. Rev. C* **21** 014001
[35] Ekström A, Baardsen G, Forssén C, Hagen G, Hjorth-Jensen M, Jansen G R, Machleidt R, Nazarewicz W, Papenbrock T, Sarich J, and Wild S M 2013 *Phys. Rev. Lett.* **110** 192502
[36] Booth G H, Thom A J W, and Alavi A 2009 *J. Chem. Phys.* **131** 054106
[37] Booth G H, Grüneis A, Kresse G, and Alavi A 2013 *Nature* **493** 365
[38] Petruzielo F R, Holmes A A, Changlani H J, Nightingale M P, and Umrigar C J 2012 *Phys. Rev. Lett.* **109** 230201
[39] ten Haaf D F B, van Bemmel H J M, van Leeuwen J M J, van Saarloos W, and Ceperley D M 1995 *Phys. Rev. B* **51** 13039
[40] Sorella S and Capriotti L 2000 *Phys. Rev. B* **61** 2599
[41] Mukherjee A and Alhassid Y 2013 *Phys. Rev. A* **88** 053622
[42] Roggero A, Mukherjee A, and Pederiva F in preparation
[43] Akmal A, Pandharipande V R, and Ravenhall D G 1998 *Phys. Rev. C* **58** 1804
[44] Gandolfi S, Carlson J, Reddy S, Steiner A W, and Wiringa R B 2013 `arXiv:1307.5815`
[45] Lattimer J M and Swesty D F 1991 *Nucl. Phys. A* **535** 331
[46] Shen G, Horowitz C J, and Teige S 2011 *Phys. Rev. C* **83** 035802
[47] Shen G, Horowitz C J, and O'Connor E 2011 *Phys. Rev. C* **83** 065808
[48] Steiner A W, Hempel M, and Fischer T 2013 *Astrophys. J.* **774** 17
[49] Shen H, Toki H, Oyamatsu K, and Sumiyoshi K 2011 *Astrophys. J. Suppl.* **197** 20
[50] Typel S, Röpke G, Klähn T, Blaschke D, and Wolter H H 2010 *Phys. Rev. C* **81** 015803
[51] Roggero A, Mukherjee A, and Pederiva F 2013 *Phys. Rev. B* **88** 115138
[52] Lynn J E and Schmidt K E 2012 *Phys. Rev. C* **86** 014324